

## A *de novo* strategy for the development of a Zn<sup>II</sup>-organic framework based luminescent “switch-on” assay for size-exclusive sensitization of the oxidised form of glutathione (GSSG) over the reduced form (GSH): insights into the sensing mechanism through DFT

Sourav Bej,<sup>[ab]</sup> Riyanka Das,<sup>[ab]</sup> Debojyoti Kundu,<sup>[ab]</sup> Tapan K. Pal<sup>[c]</sup> and Priyabrata Banerjee\*<sup>[ab]</sup>

\* E-mail: [pr\\_banerjee@cmeri.res.in](mailto:pr_banerjee@cmeri.res.in) & [priyabrata\\_banerjee@yahoo.co.in](mailto:priyabrata_banerjee@yahoo.co.in) Webpage: [www.cmeri.res.in](http://www.cmeri.res.in) & [www.priyabratabanerjee.in](http://www.priyabratabanerjee.in) Fax: +91-343-2546745; Tel: +91-343-6452220.

<sup>a</sup> Surface Engineering & Tribology Group, CSIR-Central Mechanical Engineering Research Institute, Mahatma Gandhi Avenue, Durgapur 713209, West Bengal, India.

<sup>b</sup> Academy of Scientific & Innovative Research (AcSIR), Ghaziabad – 201002, Uttar Pradesh, India

<sup>c</sup> Department of Chemistry, Pandit Deendayal Energy University, Gandhinagar- 382426, Gujarat, India

Sl. No.	Description	Entry
1	FE-SEM and EDX mapping images of Zn-CMERI	Fig. S1
2	TGA of Zn-CMERI	Fig. S2
3	Powder XRD (PXRD) studies of Zn-CMERI in different experimental conditions	Fig. S3
4	UV-vis spectra of Zn-CMERI and the co-ligands; fluorescence emission spectra of co-ligands & Zn-CMERI	Fig. S4
5	UV-vis DRS spectra of Zn-CMERI before and after interaction with GSSG & LOD plot	Fig. S5
6	Comparative literature survey of Zn-CMERI with recently reported thiol sensors	Table S1
7	Recyclability of Zn-CMERI	Fig. S6
8	FE-SEM and EDX images of Zn-CMERI before and after interaction with GSSG	Fig. S7
9	FTIR spectra of Zn-CMERI before and after interaction with GSSG	Fig. S8
10	Selectivity studies of Zn-CMERI towards different bio-hazards	Fig. S9
11	Interference experimentations of Zn-CMERI towards GSSG in presence of other biohazards	Fig. S10
12	Effect of pH on the sensing phenomenon & PXRD spectra at different pH	Fig. S11
13	N <sub>2</sub> sorption analysis with BJH plot	Fig. S12
14	HOMO-LUMO plots of co-ligand assemblies in Zn-CMERI	Fig. S13
15	Cyclic voltammograms of co-ligands	Fig. S14
16	Total energy of the asymmetric unit of Zn-CMERI before and after interaction with different biothiols	Fig. S15
17	Truth Table of Zn-CMERI with GSSG	Table S2

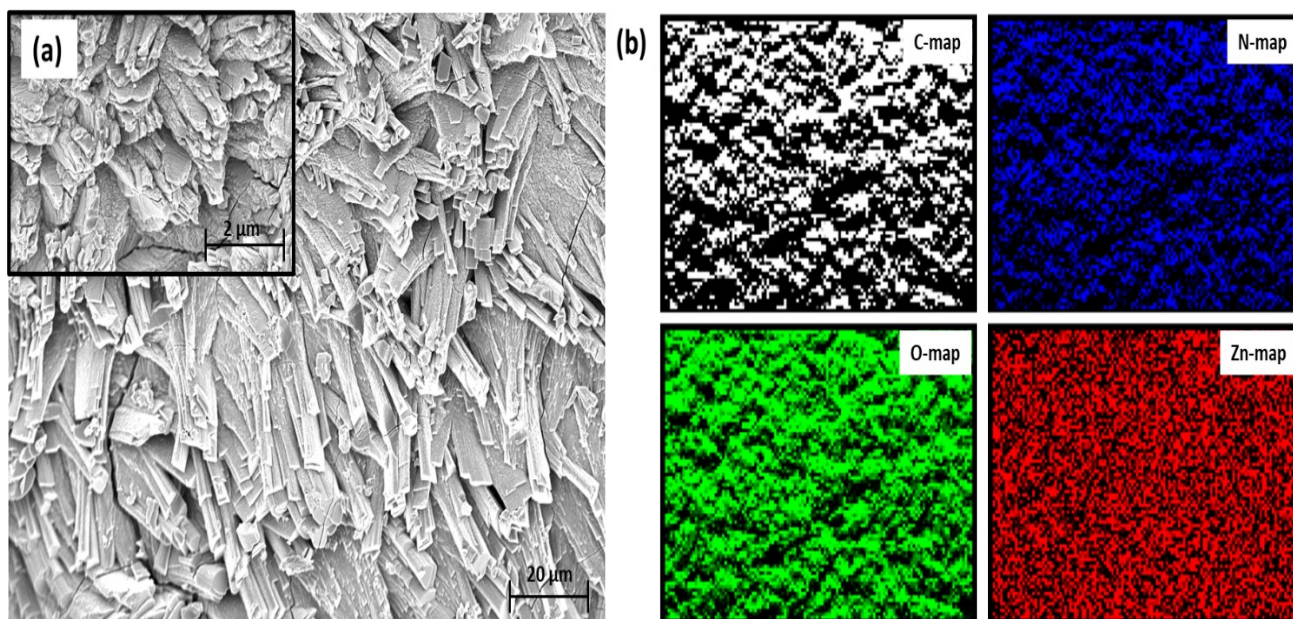


**Fig. S1** (a) FE-SEM image of Zn-CMERI, (b) EDX mapping images of carbon, nitrogen, oxygen and Zn.

#### Thermogravimetric analysis (TGA) and framework rigidity of Zn-CMERI

TGA was carried out at a temperature range between 0-600 °C with a heating rate of 5 °C/min under nitrogenous environment. The MOF is quite stable upto ~350 °C and the thermal decomposition is presumably due to release of uncoordinated guest solvent molecules. Beyond 350 °C the framework started gradual decomposition.

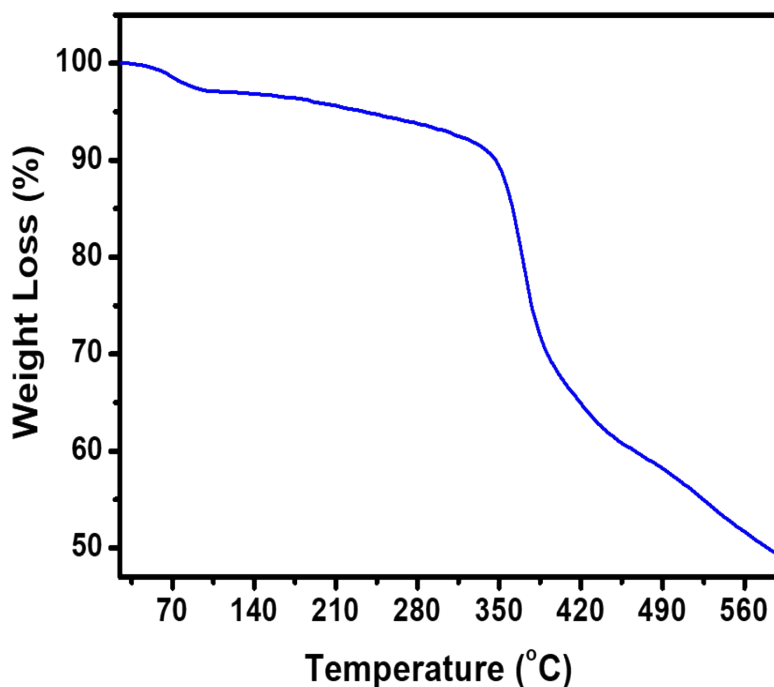


**Fig. S2** TGA curve of Zn-CMERI in nitrogen gas medium with a heating rate of 5°C/min.

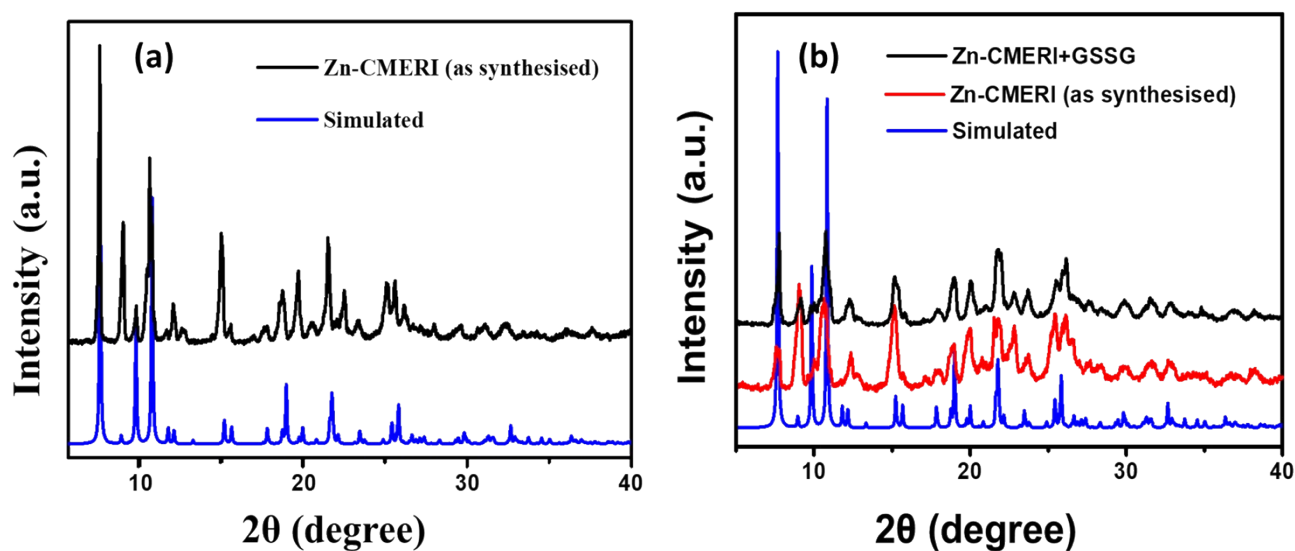


**Fig. S3** (a) PXRD pattern of as-synthesised **Zn-CMERI** with its simulated spectra, (b) Different PXRD patterns of **Zn-CMERI** confirming its structural stability

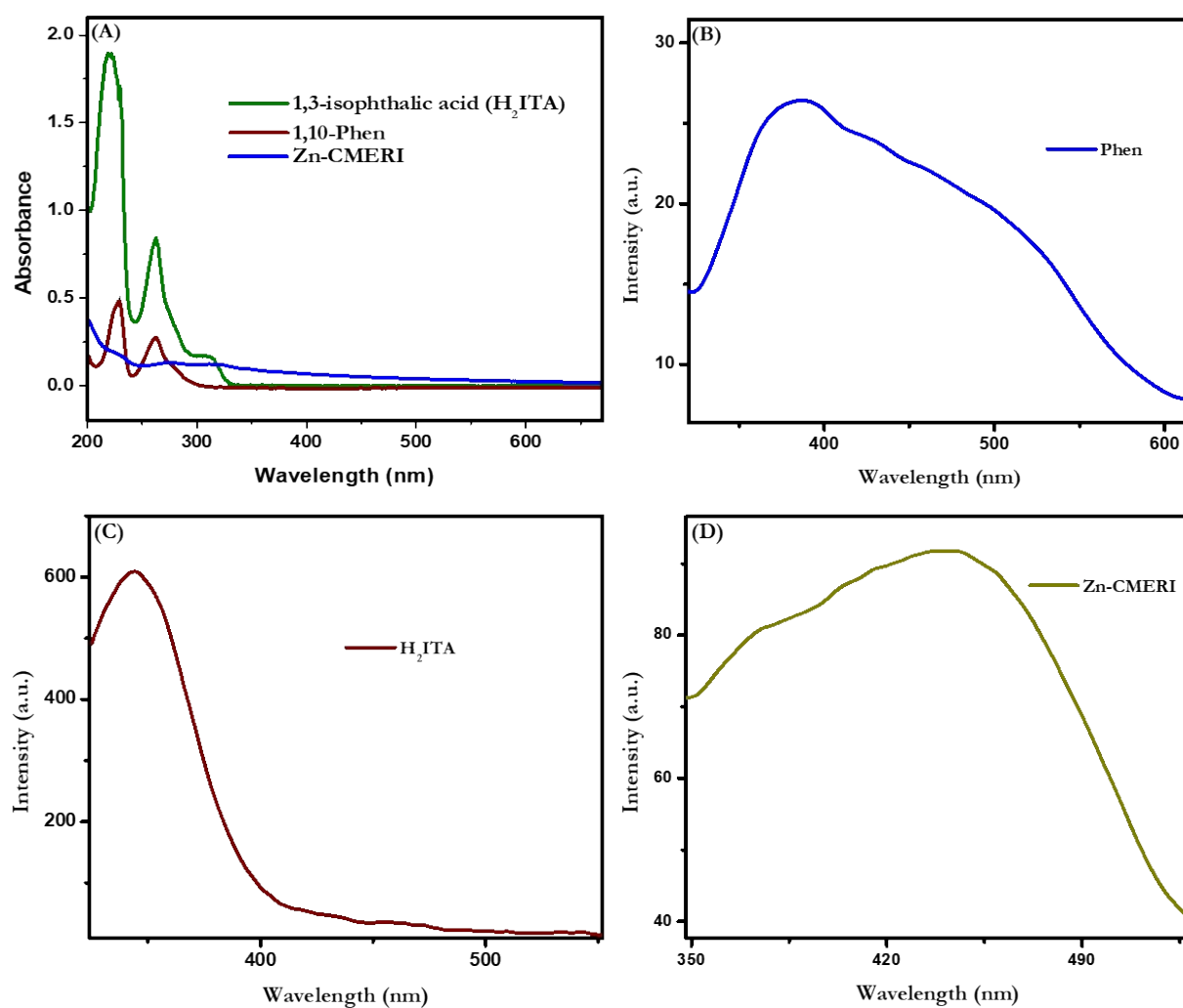


**Fig. S4** (A) UV-vis spectra of **Zn-CMERI** and the co-ligands; fluorescence emission spectra of (B) Phen, (C)  $H_2ITA$  and (D) **Zn-CMERI**.

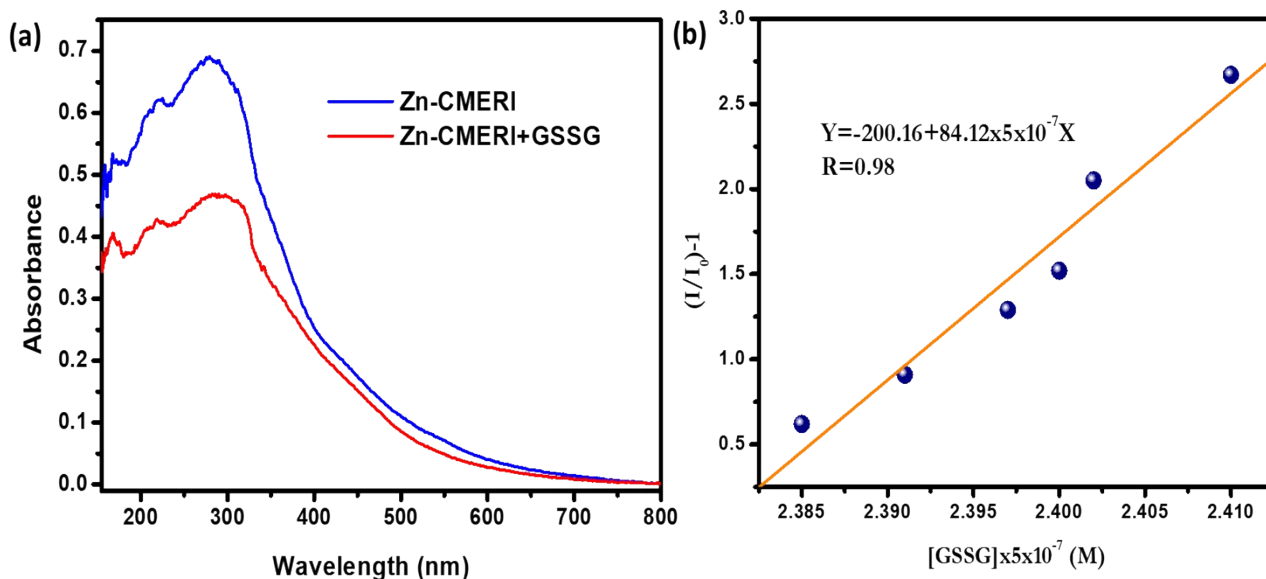


**Fig. S5 (a)** UV-vis DRS (Diffuse Reflection Spectroscopy) spectra of **Zn-CMERI** before and after interaction with GSSG, **(b)** Change of  $(I/I_0)-1$  as the linear function of the concentration of GSSG for the calculation of LOD of **Zn-CMERI** towards GSSG.

**Table S1:** Comparative literature survey of **Zn-CMERI** with recently reported chemosensors for GSSG/GSH

Sl. No.	Chemosensor	Type of analyte	Type of Chemosensor	Method of detection	pH range	LOD	Response time	Biological Applications	Application in molecular circuitry	Ref
1	PSMOF	GSH	MOF	Colorimetry	4	$\sim 0.68 \mu\text{M}$		Detection from the HeLa and LO2 cells	NA	1
2	Cu-MOF(II)	GSH	MOF	Colorimetry	7	$0.97 \mu\text{M}$		Detection from serum samples	NA	2
3	Eu(DTBA)	GSH	MOF	Fluorimetry		$0.35 \mu\text{M}$	$\sim 180 \text{ s}$	HEP 1-6 and Hacat cells in the CCK-8 assay	NA	3
4	ZIF-67	GSH	Nanosheets of a metal organic framework (MOF)	Colorimetry	5.5	$0.07 \mu\text{M}$		Detection from human serum samples	NA	4
5	Ni/Fe MOF nanosheet	GSH	Nanosheets of a metal organic framework (MOF)	Colorimetry	3	$10 \text{ nM}$		NA	NA	5

6	GSSH-2TPE		Peptide	Fluorimetry	NA	1.5 nM	~60 s	Detection from HeLa cells	NA	6
7	Eu <sup>3+</sup> /Cu <sup>2+</sup> @ UiO-67-bpydc	GSH	MOF	Fluorimetry	7.0	54.3 nM	~150 s	Detection from human serum samples	NA	7
8	UiO-66-NH <sub>2</sub> MOF	GSH	MOF	Fluorimetry	7.3	0.57 μM	NA	Detection from human serum samples	NA	8
9	CIA	GSSG	Small molecule	Fluorimetry	7.5	0.226 mM	NA	NA	NA	9
10	UiO-68-An/Ma	GSH	MOF	Fluorimetry	NA	50 μM	NA	NA	NA	10
11	Zn-CMERI	GSSG	MOF	Fluorimetry	6-8	34 nM (20.8 ppb)	~12 sec	Detection from urine and serum samples	Yes	<b>Present work</b>

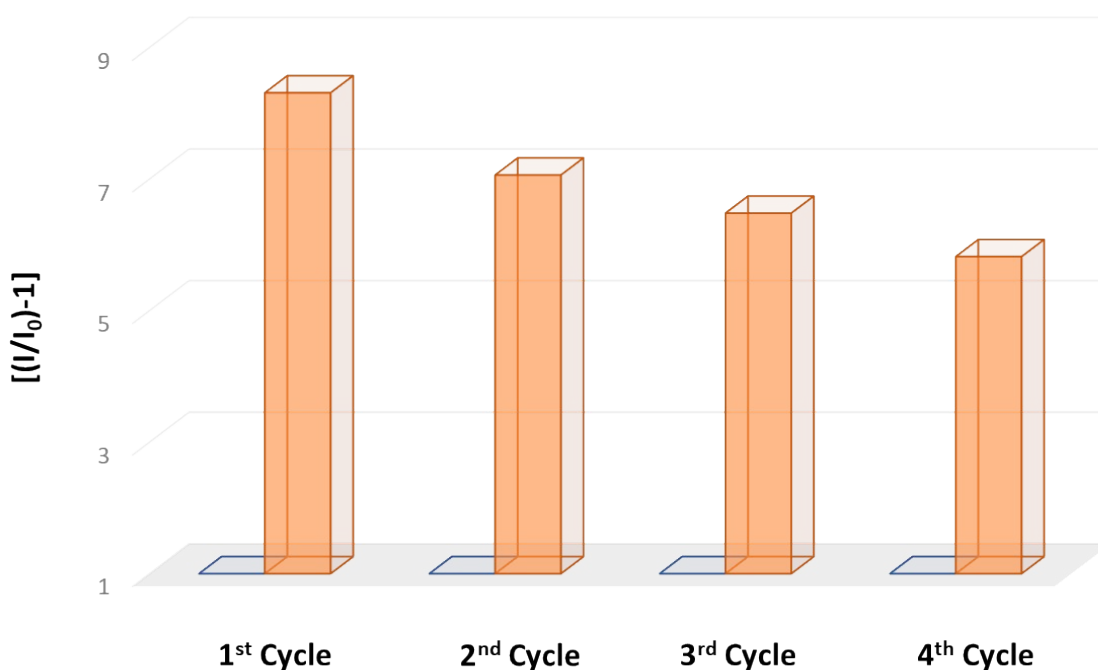


**Fig. S6** Recyclable nature of Zn-CMERI towards GSSG upto 3 cycles without any hassle.

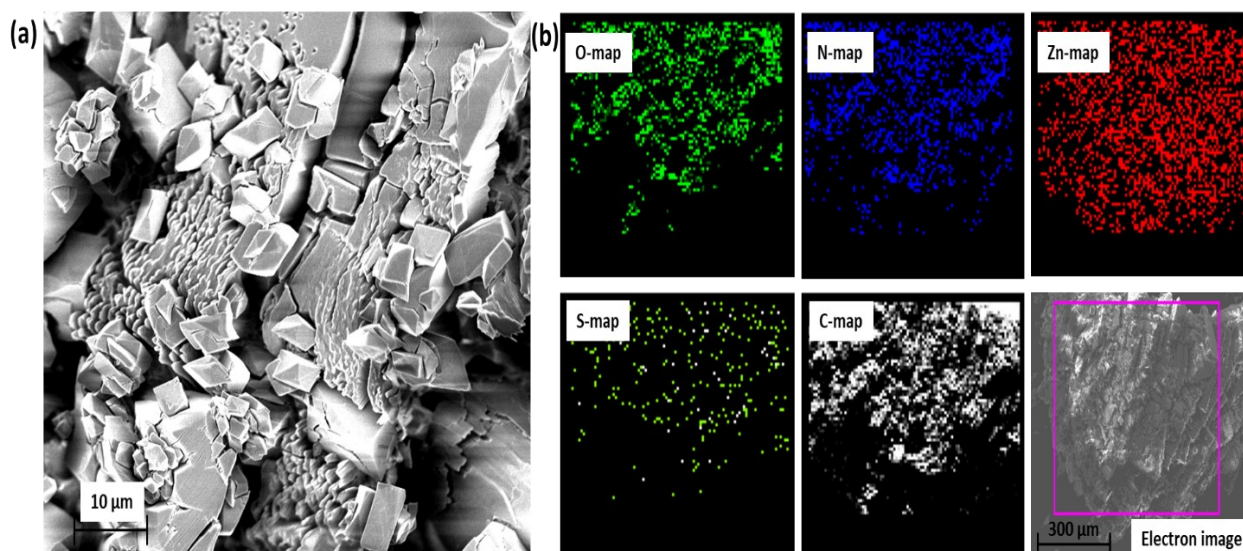


**Fig. S7** (a) FE-SEM image of unaffected needle shaped morphology of **Zn-CMERI** after interaction with GSSG, (b) EDX mapping image of **Zn-CMERI@GSSG** confirming presence of respective elements.

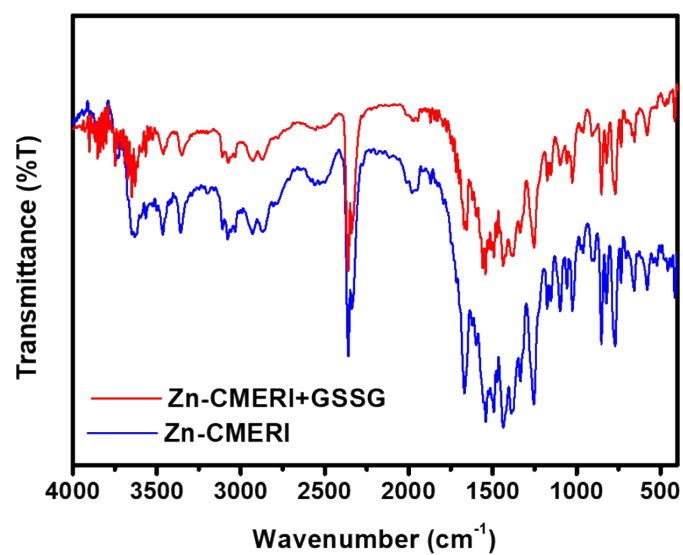


**Fig. S8** FTIR spectra of **Zn-CMERI** before and after interaction with GSSG.

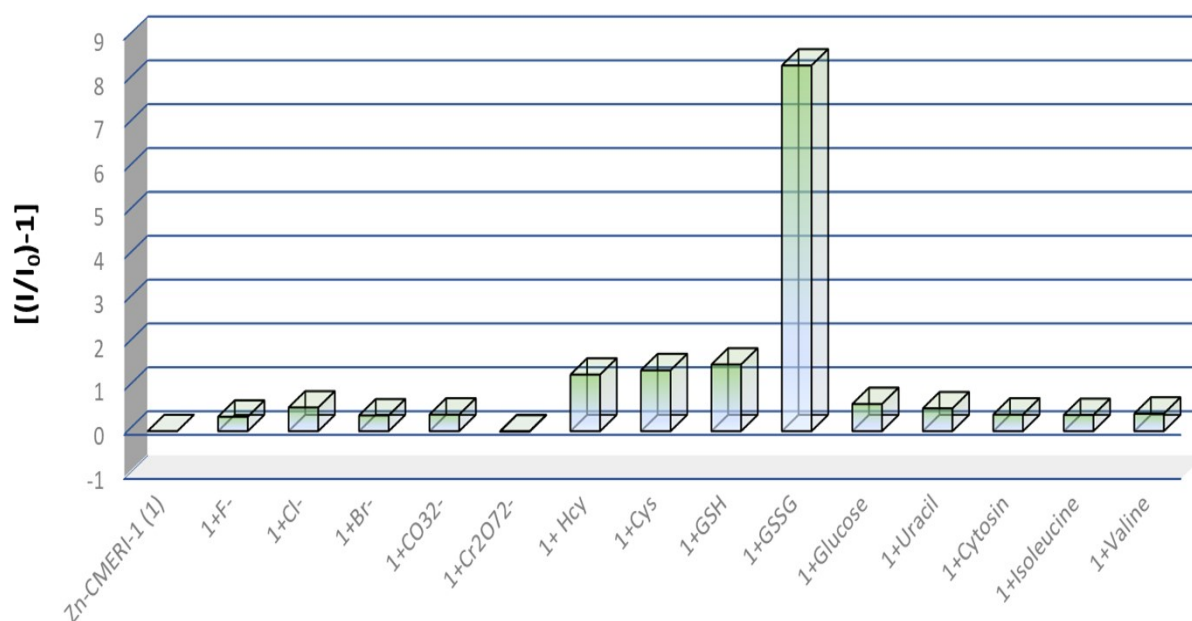


**Fig. S9** Selectivity studies of **Zn-CMERI** towards different biologically relevant interferents in similar sensing environment.

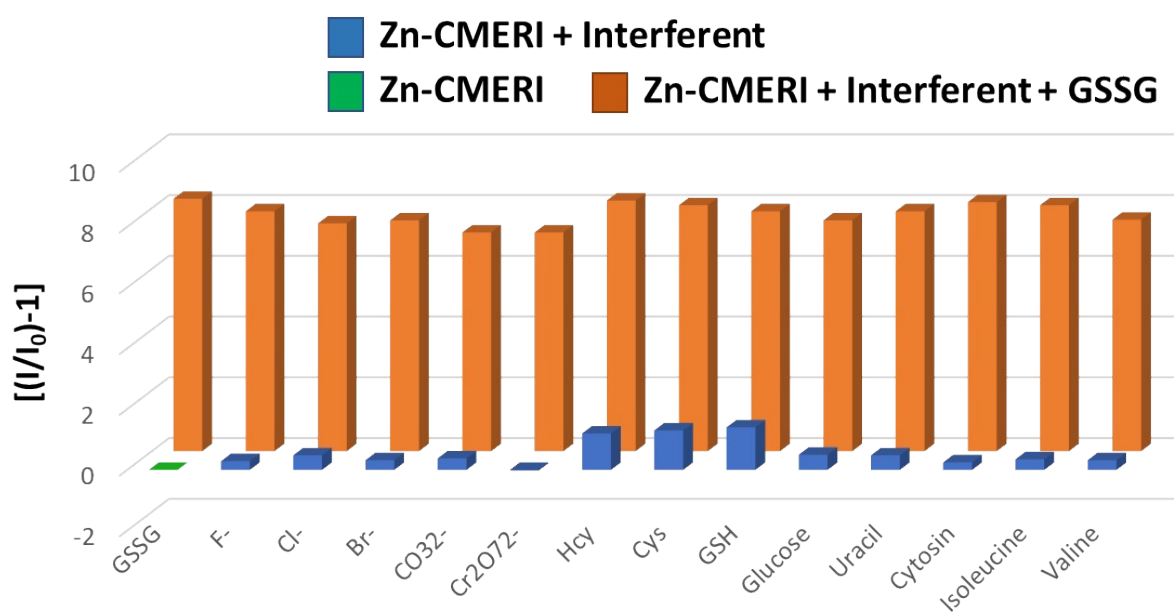


**Fig. S10** Relative fluorescence intensity of **Zn-CMERI** towards GSSG in presence of different biologically relevant interferents in similar sensing environment.

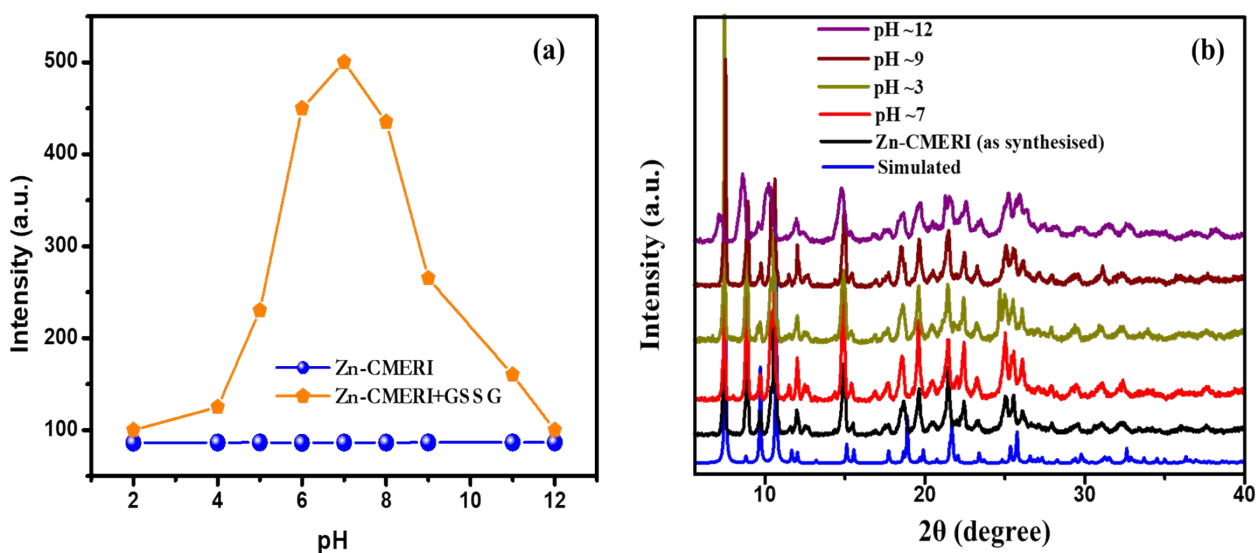


**Fig. S11** (a) Effect of fluorescence emission intensity of Zn-CMERI at 415 nm at different pH ( $\lambda_{\text{ex}}=290$  nm), (b) PXRD spectra of Zn-CMERI at different pH.

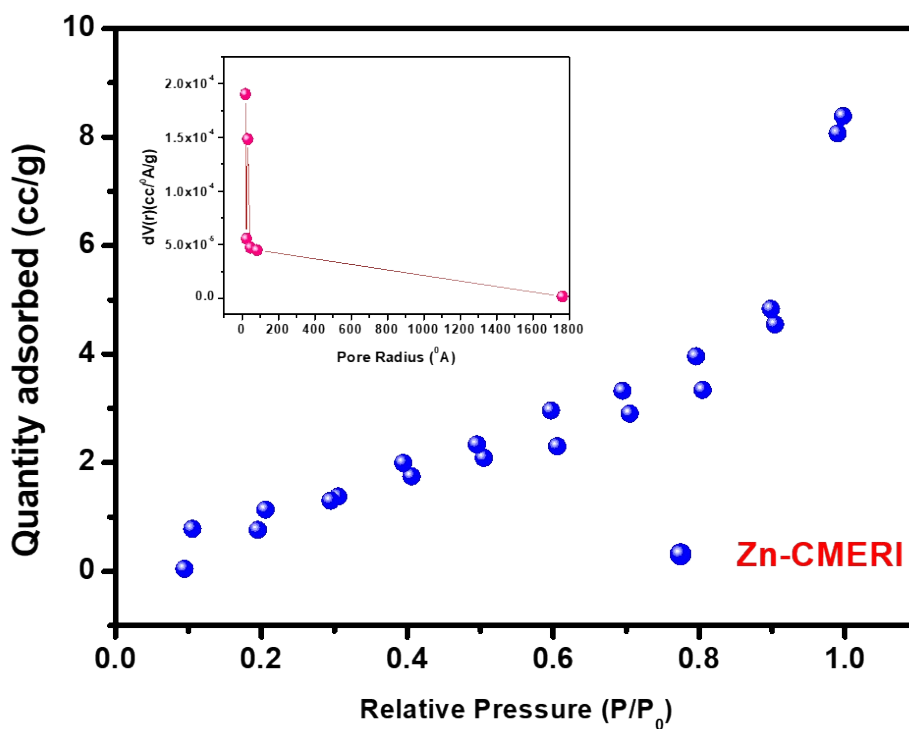


**Fig. S12** N<sub>2</sub> sorption analysis of Zn-CMERI at 77K; inset: pore size distribution of Zn-CMERI as derived from BJH method.



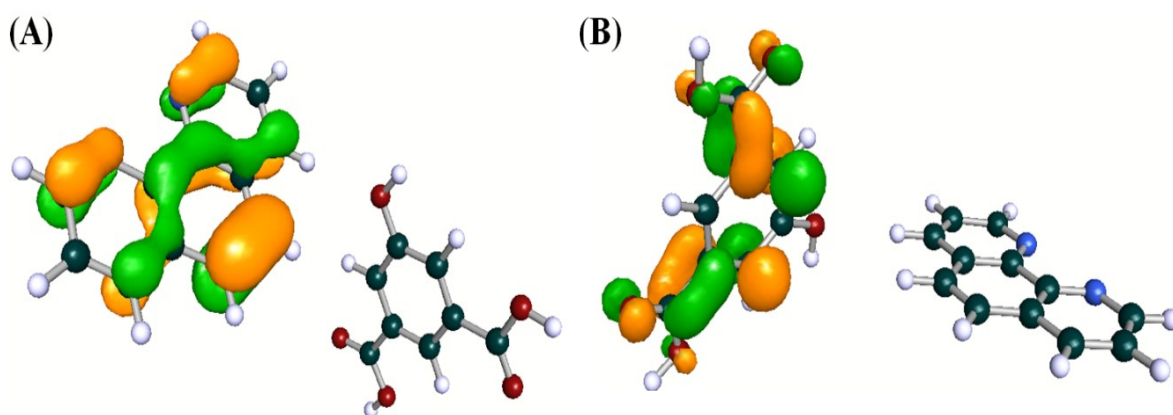


Fig. S13 (A) HOMO and (B) LUMO of the co-ligands assembly in Zn-CMERI

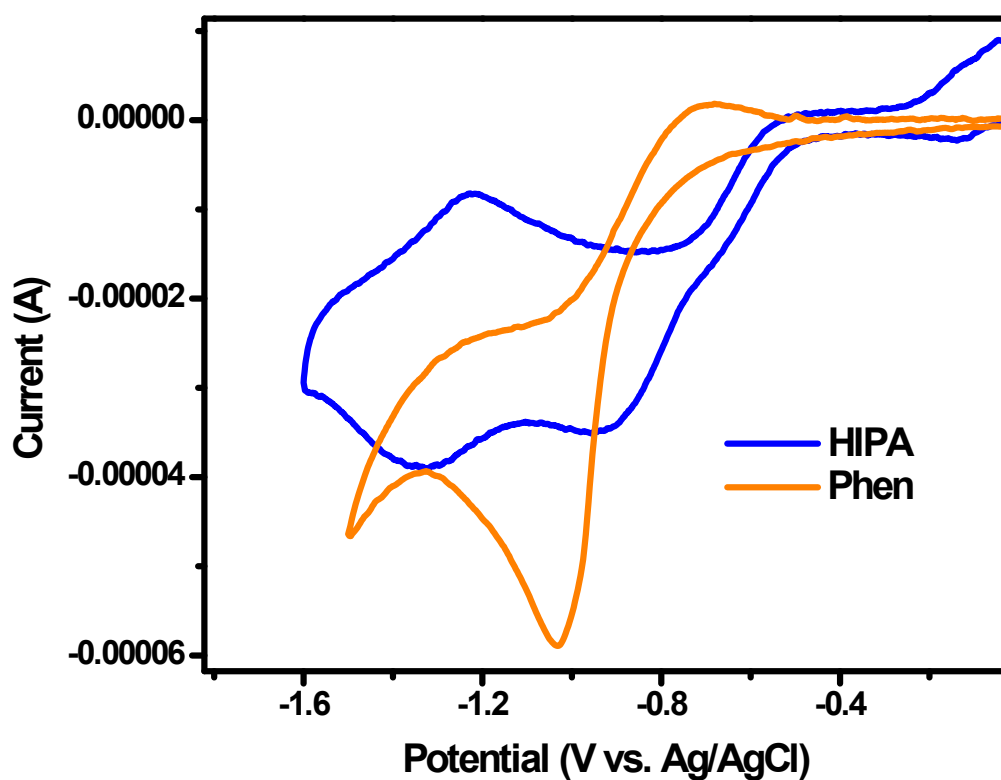
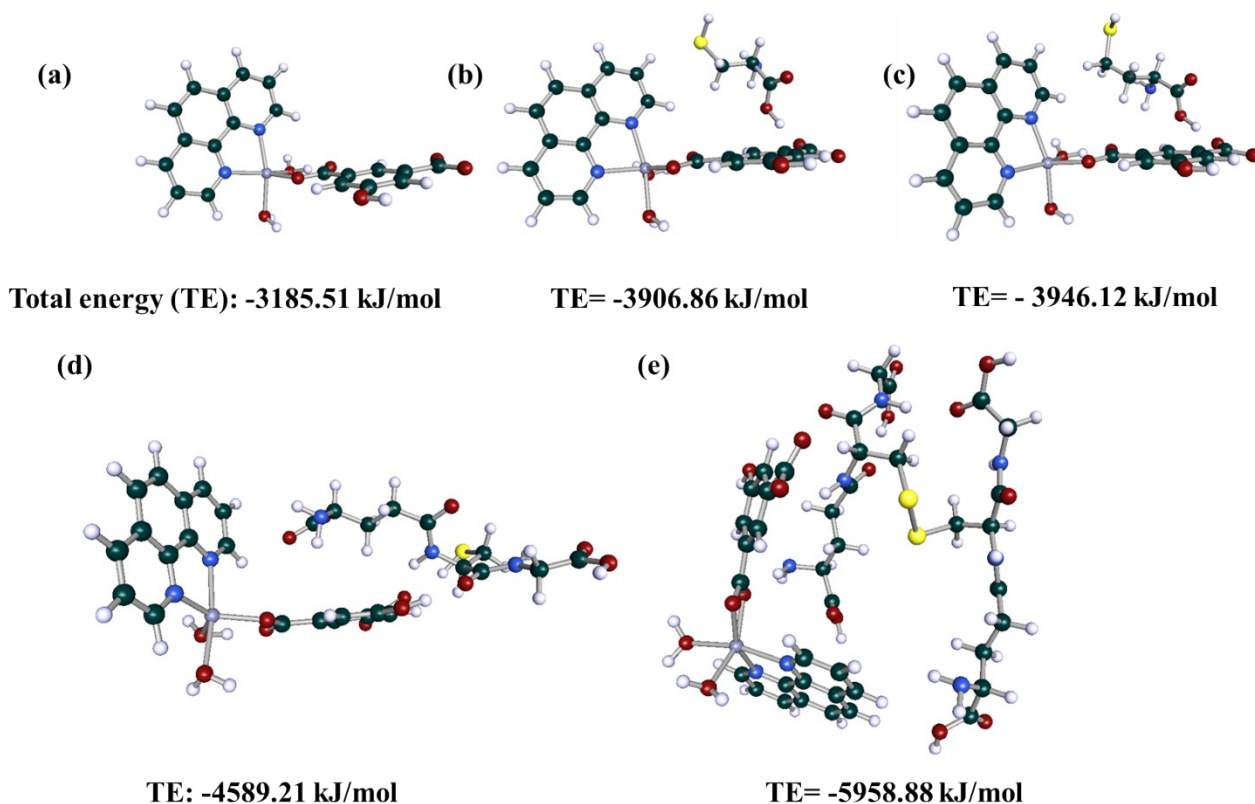


Fig. S14 Cyclic voltammogram of Phen and HIPA in acetonitrile using tetrabutylammonium hexafluorophosphate as supporting electrolyte, scan rate= 0.05 V/s.



**Fig. S15** Total energy values of (a) Zn-CMERI MOF fragment and Zn-CMERI MOF fragment with (b) Cys, (c) Hcy, (d) GSH and (e) GSSG respectively.

**Table S2** Truth table presenting output at the emission wavelength of 415 nm for the chemosensor, Zn-CMERI in presence of the targeted analyte, GSSG

IN 1 (Zn-CMERI)	IN2 (GSSG)	OUT1 (415 nm)
0	0	0
0	1	0
1	0	0
1	1	1

## References

- 1 Y. Liu, M. Zhou, W. Cao, X. Wang, Q. Wang, S. Li and H. Wei, *Anal. Chem.*, 2019, **91**, 8170–8175.
- 2 J. Wang, W. Li and Y.-Q. Zheng, *Analyst*, 2019, **144**, 6041–6047.
- 3 M. M. Zhu, Y. P. Liu, C. Xia, H. R. Zeng, S. Hu, D. Y. Jiang, G. H. Zhou and H. L. Li, *SSRN Electron. J.*, , DOI:10.2139/ssrn.4084528.
- 4 Y. Zhang, C. Dai, W. Liu, Y. Wang, F. Ding, P. Zou, X. Wang, Q. Zhao and H. Rao, *Microchim. Acta*, 2019, **186**, 340.
- 5 Q. Li, Q. Wang, Y. Li, X. Zhang and Y. Huang, *Anal. Methods*, 2021, **13**, 2066–2074.
- 6 S. Gui, Y. Huang, Y. Zhu, Y. Jin and R. Zhao, *ACS Appl. Mater. Interfaces*, 2019, **11**, 5804–5811.
- 7 J. Zhu, Y. Tang, Y. Yang, B. Li, Y. Cui and G. Qian, *Microporous Mesoporous Mater.*, 2019, **288**, 109610.

- 8 N. Wang, M. Xie, M. Wang, Z. Li and X. Su, *Talanta*, 2020, **220**, 121352.
- 9 P. Ravichandiran, D. S. Prabakaran, N. Maroli, A. Boguszewska-Czubara, M. Masłyk, A. R. Kim, B. Chandrasekaran and D. J. Yoo, *Anal. Chim. Acta*, 2021, **1181**, 338896.
- 10 B. Gui, Y. Meng, Y. Xie, J. Tian, G. Yu, W. Zeng, G. Zhang, S. Gong, C. Yang, D. Zhang and C. Wang, *Adv. Mater.*, 2018, **30**, 1802329.